

# Infrared characterization studies of poly-crystalline silicon annealed in a nitrogen atmosphere

D. GUPTA, B. AWASTHY, S. P. VARMA

National Physical Laboratory, Dr K. S. Krishnan Road, New Delhi 110012, India

A systematic study of the effect of annealing treatment in a nitrogen atmosphere on the oxygen and carbon impurities present in solar grade polysilicon has been conducted in the spectral region  $4000\text{--}400\text{ cm}^{-1}$  employing infrared spectroscopy. Thermal treatment was provided for 30 min at temperatures varying from  $100\text{--}1300^\circ\text{C}$ . Results of the present study are in conformity with the reported annealing results on resistivity and photoconductivity.

## 1. Introduction

Polycrystalline silicon, a suitable material for cheap solar cells, contains high contents of impurities because of the presence of a large number of structural defects (grain boundaries and dislocations). The role of oxygen and carbon impurities present in monocrystalline silicon during thermal treatment has been studied systematically [1–6]. However, in the case of polysilicon [7–10], the behaviour of these impurities is more complicated because of their segregation close to structural defects, especially the grain boundaries. This affects the conduction mechanism to a considerable extent [7, 8, 10]. Because segregated oxygen is infrared invisible at room temperature, thermal treatment provides realistic evaluation of oxygen present in polysilicon [9]. Hence, a systematic study of the effect of annealing treatment in a nitrogen atmosphere on the oxygen and carbon impurities present in polysilicon, has been conducted employing infrared spectroscopic techniques.

## 2. Experimental procedure

The polycrystalline silicon under study was prepared in the laboratory by chemical vapour deposition (CVD) technique. The high-purity  $\text{SiHCl}_3$  was reduced in the presence of hydrogen and was made to deposit over a resistance-heated silicon filament enclosed in a quartz reactor [11]. All the infrared spectra were obtained at room temperature using an infrared spectrophotometer, Perkin Elmer 399, operating in the spectral region  $4000\text{--}400\text{ cm}^{-1}$  ( $2.5\text{--}25\text{ }\mu\text{m}$ ). The ASTM method [12] was employed for the evaluation of the concentration of oxygen and carbon impurities. The thickness of the samples used was kept to  $1\text{--}5\text{ mm}$ . The samples were annealed in a nitrogen atmosphere (ultrahigh purity) for 30 min at temperatures varying from  $100\text{--}1300^\circ\text{C}$ . The annealed samples were cooled slowly to ambient temperature by gradually decreasing the furnace temperature.

## 3. Results and discussion

Fig. 1 shows the infrared spectrum of polysilicon in the spectral region  $4000\text{--}400\text{ cm}^{-1}$  without any thermal treatment. The bands appearing at  $1108$  and  $615\text{ cm}^{-1}$  correspond to Si–O and Si–C modes, respectively, and are generally employed to evaluate the oxygen and carbon contents in silicon. The concentrations of oxygen and carbon in polysilicon as determined by the ASTM method [12] are  $1.327 \times 10^{18}$  and  $4.14 \times 10^{17}$  atoms  $\text{cm}^{-3}$ , respectively. These high contents of impurities are responsible for the reduction in the efficiency of a solar cell produced from polysilicon, compared to that produced from monocrystalline silicon.

The results of the variation of oxygen and carbon concentrations and frequencies of Si–O and Si–C modes with different annealing temperatures are presented in Table I. Fig. 2 shows spectral changes occurring in the finger print region of  $1200\text{--}400\text{ cm}^{-1}$  due to annealing treatment. It has been observed that with increasing annealing temperature, while the carbon concentration does not vary considerably, oxygen content is enhanced to a reasonable extent. The temperature dependence of oxygen concentration has also been reported by Boyed *et al.* [6] in monocrystalline silicon. Further, the position of the Si–C band does not change significantly due to annealing, whereas the Si–O mode becomes softened. Schroder *et al.* [3] have also reported the shift in position of Si–O mode during thermal treatment in single-crystal silicon. Carbon is distributed uniformly at substitutional positions and has a nearly constant concentration at all the annealing temperatures. This means that there is no migration of carbon from grain boundaries to the grain with increase in annealing temperature. This is further confirmed by the fact that there is no considerable shift in the position of the Si–C band due to annealing effects. The diffusion coefficient of carbon in silicon at  $700^\circ\text{C}$  is nearly zero, and at  $1000^\circ\text{C}$  is  $\approx 10^{-13}\text{ cm}^2\text{ s}^{-1}$  which is small compared to that of

TABLE I Oxygen and carbon concentrations and frequencies of Si-O and Si-C modes at different annealing temperatures

Serial no.	Temperature (°C)	Concentration ( $10^{17}$ at units)		Frequency ( $\text{cm}^{-1}$ )	
		Oxygen	Carbon	Si-O	Si-C
1	Ambient	13.27	4.14	1108	615
2	100	13.52	3.81	1106	605
3	300	13.43	4.05	1105	606
4	500	13.43	4.02	1105	604
5	700	13.57	3.88	1100	606
6	800	14.69	4.05	1093	606
7	900	15.32	3.81	1085	607
8	1000	16.51	4.07	1080	607
9	1100	16.55	4.05	1080	604
10	1300	16.78	3.99	1080	605

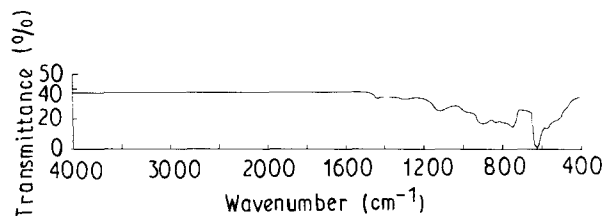


Figure 1 Infrared spectrum of polycrystalline silicon without annealing treatment.

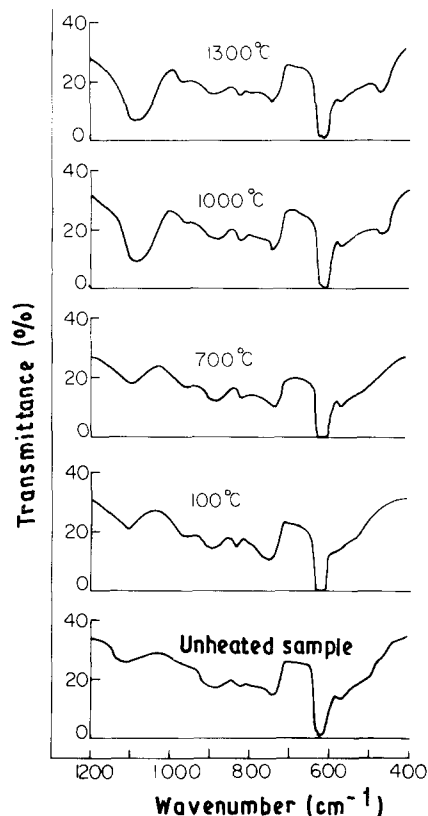


Figure 2 Infrared spectra of annealed polycrystalline silicon in the finger print region of  $1200\text{--}400\text{ cm}^{-1}$ .

oxygen ( $\approx 10^{-12}\text{ cm}^2\text{s}^{-1}$ ) [14]. A weak band has appeared at  $960\text{ cm}^{-1}$  in annealed samples which possibly indicates the presence of some nitrogen [15].

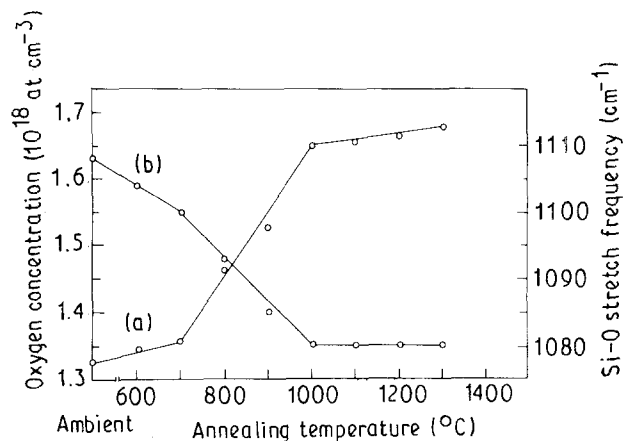


Figure 3 Plots of (a) concentration of oxygen, and (b) Si-O stretching frequency versus annealing temperature.

However, annealing effects seem to be important only for oxygen in the present study.

The behaviour of oxygen with thermal treatment is better explained by the plots shown in Fig. 3. Curve (a) in Fig. 3 shows the plot of oxygen concentration against the annealing temperature. The oxygen concentration is considerably enhanced between  $700^\circ$  and  $1000^\circ\text{C}$ . However, below  $700^\circ\text{C}$  and above  $1000^\circ\text{C}$ , the variation in oxygen content is very small. This is explained on the basis that segregated oxygen precipitates are dissolved upon annealing treatment between  $700^\circ$  and  $1000^\circ\text{C}$ . Grain boundaries are acting as a source of oxygen, being diffused into grains in polysilicon. The diffusion coefficient of oxygen in silicon [12] is  $8 \times 10^{-16}\text{ cm}^2\text{s}^{-1}$  at  $700^\circ\text{C}$  and  $2 \times 10^{-12}\text{ cm}^2\text{s}^{-1}$  at  $1000^\circ\text{C}$ . Segregated oxygen is normally not detected by infrared spectroscopy. Only oxygen at well-defined positions (such as the interstitial position) can be measured by this means. The dissolution of segregated oxygen leads to its homogenization and its placement at the interstitial position through the bulk of the material [9]. The small variation in oxygen content below  $700^\circ\text{C}$  and above  $1000^\circ\text{C}$  is understandable, because the process of dissolution of segregated oxygen does not start below  $700^\circ\text{C}$ , and above  $1000^\circ\text{C}$  there is no further dissolution of segregated oxygen. The diffusion coefficient of oxygen in silicon is very low ( $\approx 10^{-16}\text{ cm}^2\text{s}^{-1}$ ) [12] below  $700^\circ\text{C}$ . However, above  $1000^\circ\text{C}$ , though the diffusion coefficient is high ( $\approx 10^{-12}\text{ cm}^2\text{s}^{-1}$ ) there is no concentration gradient and only a marginal migration of oxygen takes place from grain boundaries to grains. This provides an interpretation of the variation of oxygen content at different annealing temperatures. The maximum oxygen content measured at  $1300^\circ\text{C}$  is  $1.678 \times 10^{18}\text{ atoms cm}^{-3}$ . The content of segregated oxygen in the samples under study has been determined as  $3.5 \times 10^{17}\text{ atoms cm}^{-3}$ .

The variation of frequency of the Si-O mode with annealing temperature is shown in Fig. 3b. Curve b in Fig. 3 seems to be mirror image of Curve a. While there is enhancement of oxygen content with increase in annealing temperature, the Si-O mode frequency is shifted to a lower wave number. The position of the

Si–O mode in unannealed polysilicon is  $1108\text{ cm}^{-1}$  and shifts to  $1100\text{ cm}^{-1}$  at  $700^\circ\text{C}$  and  $1080\text{ cm}^{-1}$  at  $1000^\circ\text{C}$ . The shift of Si–O mode towards a lower wave number leads to a reduction in the strength of a bond between silicon and oxygen. In other words, the Si–O mode becomes softened [16] and the shift of  $28\text{ cm}^{-1}$  in position of Si–O frequency may be explained by the dependence of mobility of oxygen on annealing temperature. As the temperature rises, the interstitial oxygen atoms become mobile and are trapped by substitutional carbon to form simple carbon–oxygen pairs [17]. The softening of the Si–O mode is interpreted as a modification of the absorption of interstitial oxygen at  $1108\text{ cm}^{-1}$ , because of the existence of carbon–oxygen pairs [3, 16].

The present results based on the infrared studies are in conformity with the annealing results on resistivity and photoconductivity reported by Jain *et al.* [10]. Their studies were conducted in the temperature range  $900\text{--}1100^\circ\text{C}$  which is necessary for processing the material for solar-cell fabrication, and their results were found to be independent of the annealing environment. Jain *et al.* [10] reported that the value of  $\alpha$  (the ratio of resistivities of annealed and unannealed samples) increased with increasing annealing temperature and attributed it primarily to the bending of electronic bands at the grain boundaries [18], and not to oxygen precipitation. Results of the present study also indicate that at higher annealing temperatures (above  $700^\circ\text{C}$ ), oxygen does not exist in precipitate forms but is dissolved uniformly within the bulk of the material [9].

A better understanding of the earlier results of Jain *et al.* [10] could be achieved from the present results. They have shown that the photoconductivity ratio,  $\beta$ , of annealed and unannealed samples also varies more or less like the resistivity ratio,  $\alpha$ , and these variations in  $\beta$  may be due to the acceptor traps at the grain boundaries [18] whose concentration seems to increase with annealing temperature. However, the present results predict that the increase in photoconductivity may be due to mobile oxygen atoms becoming electrically active centres with annealing treatment.

In a recent publication, Borghesi *et al.* [19] reported an absorption peak at  $1230\text{ cm}^{-1}$  in Czochralski-grown silicon and attributed it to the existence of  $\text{SiO}_2$  precipitates in the sample. This absorption peak at  $1230\text{ cm}^{-1}$  due to precipitates was missing in the infrared spectra of the present study and it may be because the absorption peak at  $1230\text{ cm}^{-1}$  is due to longitudinal optical phonon vibrations of  $\text{SiO}_2$  pre-

cipitates which is normally infrared inactive, but can become active for particles in platelet shape and with size  $\leq 0.36\text{ }\mu\text{m}$ . Thus, the appearance of the  $1230\text{ cm}^{-1}$  absorption band seems to be dependent on both the size and the shape of particles in the silicon matrix.

## Acknowledgements

The authors thank the Head, Physico-Mechanical Standards Division and the Director for their permission to publish this work.

## References

1. J. J. QIAN, Z. G. WANG, S. K. WAN and L. Y. LIN, *J. Appl. Phys.* **68** (1990) 954.
2. A. HARA, T. FUKUDA, T. MIYABO and L. HIRAI, *Appl. Phys. Lett.* **54** (1989) 626.
3. D. K. SCHRODER, C. S. CHEN, J. S. KANG and X. D. SONG, *J. Appl. Phys.* **63** (1988) 136.
4. A. R. BROWN, M. CLAYBOURN, R. MURRAY, P. S. NANDRA, R. C. NEWMAN and J. H. TUCKER, *Semicond. Sci. Technol.* **3** (1988) 591.
5. F. SHIMURA, R. S. HOCKETT, D. A. REED and D. H. WAYNE, *Appl. Phys. Lett.* **47** (1985) 794.
6. I. W. BOYED, T. D. BINNIE, J. I. B. WILSON and M. J. COLLES, *J. Appl. Phys.* **55** (1984) 3061.
7. K. PARK, S. BATRA, J. LIN, S. YOGANATHAN, S. BANERJEE, J. LEE, S. SUN, J. YEARGAIN and G. LUX, *Appl. Phys. Lett.* **56** (1990) 2325.
8. K. SAGARA and E. MURAKAMI, *ibid.* **54** (1989) 2003.
9. B. PIVAC, *J. Phys. D Appl. Phys.* **21** (1988) 1241.
10. G. C. JAIN, B. C. CHAKRAVARTY and A. PRASAD, *J. Appl. Phys.* **52** (1981) 3700.
11. S. PIZZINI, *Solar Energy Mater.* **6** (1982) 253.
12. "Annual Book of ASTM Standards", Part 43 F 120-75, R. P. Lukens, J. L. Cornillot and R. A. Priemon eds. (American Society for Testing and Materials, Philadelphia, PA, 1981) p. 533.
13. B. O. KOLBESEN and A. MUHLBAUER, *Solid State Electron.* **25** (1982) 759.
14. H. F. WOLF (ed.) "Silicon Semiconductor Data", Signetics Corporation (Pergamon Press, Oxford, London, 1969).
15. Y. ITOH, T. NOZAKI, T. MASUI and T. ABE, *Appl. Phys. Lett.* **47** (1985) 488.
16. A. SMAKULA and J. KALNAJS, *J. Phys. Chem. Solids* **6** (1958) 46.
17. R. C. NEWMAN and R. S. SMITH, *ibid.* **30** (1969) 1493.
18. E. MUNOZ, J. M. BOIX, J. LLABRES, J. MONICO and J. PIQUERAS, *Solid State Electron.* **17** (1974) 439.
19. A. BORGHESI, M. GEDDO and B. PIVAC, *J. Appl. Phys.* **69** (1991) 7251.

Received 24 September 1991

and accepted 30 March 1992